J|A|C|S
COMMUNICATIONS

Published on Web 04/05/2003

Self-Assembly of Microporous Manganese Oxide Octahedral Molecular Sieve Hexagonal Flakes into Mesoporous Hollow Nanospheres

Jikang Yuan,[†] Kate Laubernds,[‡] Qiuhua Zhang,[||] and Steven L. Suib*[,†,‡,§]

Department of Chemistry, Department of Chemical Engineering, and Institute of Materials Science, Unit 3060, 55 North Eagleville Road, University of Connecticut, Storrs, Connecticut 06269-3060

Received November 22, 2002; E-mail: suib@uconnvm.uconn.edu

Assembly of transition metal oxide nanoparticles to form ordered structures is of great interest in the area of materials science. The ability to synthesize uniform hollow nanospheres with diameters ranging from nano- to microscale dimensions is desirable. These structures can be used as catalysts, potential drug carriers, fillers, and photonic crystals.[1] Methods to synthesize these materials include the use of various template precursors, such as spherical silica, polystyrene spheres, and block copolymer micelles.[2] These preparations often require removal of the template after synthesis utilizing separation techniques such as acid or base etching and calcination.[3] Here we report on a simple self-assembly synthesis of manganese oxide mesoporous hollow nanospheres, which are composed of porous γ-MnO_2 hexagonal nanoflakes.

Manganese oxide structures can form mixed-valent octahedral molecular sieves (OMS). These OMS materials have extensive applications in energy storage applications, as acid catalysts, and in ion-exchange processes.[4,5] Various types of manganese oxides with fibrous and flaky morphologies have been synthesized.[6] An electrochemically active form of manganese oxides is γ-MnO_2; this form of Mn oxide has been commercially used as cathodic materials in alkaline batteries. γ-MnO_2 is a ramsdellite matrix with randomly distributed intergrowth microdomains of pyrolusite, which are constructed of MnO_6 octahedral units with edge or corner sharing.[7] Conventionally, γ-MnO_2 was prepared by electrolysis (EMD), redox reactions, or disproportionation. However, to the best of our knowledge, the γ-MnO_2 synthesized using the above methods has irregular morphologies and surface areas no higher than 80 m^2/g.[8] MnO_2's electrochemical performance is greatly affected by morphology, surface area, and the pore size distribution.[9]

Diluted $MnSO_4 \cdot 4H_2O$ was reacted with permanganic acid (pH = 2.50) at room temperature to synthesize γ-MnO_2. Fresh permanganic acid must be prepared prior to use and is made by reacting sulfuric acid and barium manganate.[10] To prevent undesirable byproducts, barium manganate was chosen as the manganate salt. Barium sulfate is insoluble in water, thus preventing metallic ions from entering synthetic structures (see eqs 1 and 2).

$$3BaMnO_4 + 3H_2SO_4 \rightarrow 3BaSO_4 + MnO_2 + 2HMnO_4 + 2H_2O \quad (1)$$

$$2HMnO_4 + 2H_2O + 3MnSO_4 \rightarrow 5MnO_2 + 3H_2SO_4 \quad (2)$$

First 2.67 mL of 4.23 M H_2SO_4 was added dropwise to 100 mL of 0.1 M $BaMnO_{4(aq)}$. After being vigorously stirred at room temperature for 10 min, the solution was centrifuged and decanted. The resultant pink solution was added dropwise to 400 mL of 0.02 M $MnSO_4 \cdot H_2O$ while being rapidly stirred for 12 h at room temperature. The slurry formed was filtered and washed with deionized water at least four times and then dried in air at 120 °C for an additional 12 h. Analysis of the product was performed by ion chromatography (IC), X-ray diffraction (XRD), adsorption measurements, thermal gravimetric analysis (TGA), scanning electron microscopy (SEM), transmission electron microscopy (TEM), and energy-dispersive X-ray spectroscopy (EDX).

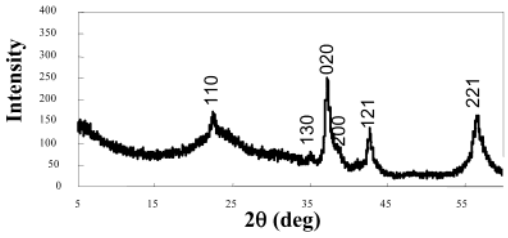

Figure 1. X-ray diffraction (XRD) pattern of γ-MnO_2 hollow nanospheres.

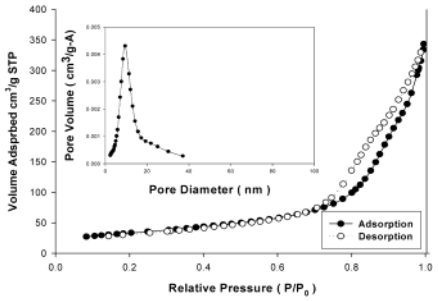

Figure 2. N_2 adsorption/desorption isotherms and pore size distributions (insert) of hollow γ-MnO_2 nanospheres.

The phase of the product was identified by XRD using a Scintag X-ray diffractometer with Cu Kα radiation (λ = 0.15406 nm) operating at 45 kV and 40 mA. The observed peaks in the XRD pattern correlate to pure phase, hexagonal γ-MnO_2 (Figure 1). The lattice parameters for the hexagonal γ-MnO_2 are $a = b = 9.65$ Å and $c = 4.43$ Å. A space group for this structure is not applicable due to the combination of different tunnel geometries.

Elemental analysis was performed by IC and EDX to confirm that neither sulfate ions nor sulfur was incorporated into the structure; results from both techniques showed only trace amounts (less than 1%) of sulfate (IC) or sulfur (EDX) present.

The pore size distribution of the nanoparticles was calculated from nitrogen desorption using the BJH (Barrett−Joyner−Halenda) model. The results show a narrow distribution centered at 10 nm (Figure 2). The type III isotherm observed is similar to that of γ-MnO_2 prepared by other means and is consistent with platelet materials such as clays.[11] The BET surface area of the γ-MnO_2 hollow nanospheres calculated from N_2 adsorption is 130 m^2/g. This is the highest surface area observed for synthesized γ-MnO_2.

[†] Institute of Materials Science.
[‡] Department of Chemistry.
[§] Department of Chemical Engineering.
[||] Present address: Carus Co. Ltd.

10.1021/ja0294459 CCC: $25.00

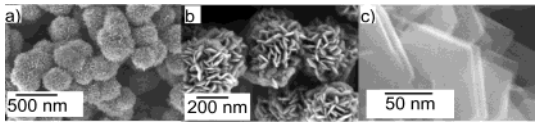

Figure 3. HR-SEM images of γ-MnO_2 nanospheres. The images increase in magnification from (a) to (c). (c) shows the nanospheres are composed of hexagonal flakes of γ-MnO_2 single crystals.

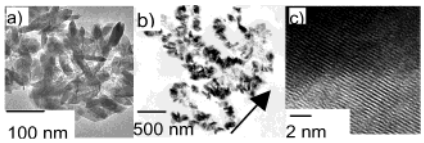

Figure 4. TEM bright field images of γ-MnO_2 hollow nanospheres. (b) is a cross-sectional view of the nanosphere prepared by microtomy; the arrow indicates cut direction. (c) is a view perpendicular to the hexagonal flakes of γ-MnO_2 corresponding to the 110 plane, $d = 4.04$ Å.

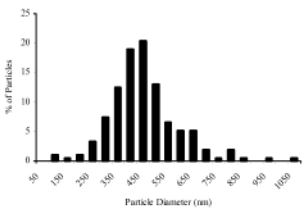

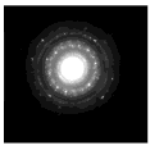

ring	d-spacing Å (plane)
1	4.02 (110)
2	2.68 (020)
3	2.17 (121)
4	1.67 (221)

Figure 5. (a) Particle size distribution for nanospheres; (b) ring pattern of hollow nanospheres with corresponding *d*-spaces (ring number increases as you move away from the transmitted spot).

These nanospheres have three levels of structure. Each independent flake is a microporous structure (intergrowth of 1×1 and 1×2 tunnels), the self-assembled structure results in additional porosity from the empty core, and the third porosity results from the physical packing of flakes in the shell. The 1×1 tunnel of pyrolusite and the 1×2 tunnel of ramsdellite (2.3 Å $\times$ 2.3 Å and 2.3 Å $\times$ 4.6 Å) dictate the microporosity of the flakes.

The density of the nanospheres is controlled by the rate of addition of the permanganic acid. When it is added dropwise, hollow nanospheres are produced (shell thickness = 75 nm), and when it is added quickly, solid nanospheres are observed. The diameter and pore size of the structures are dictated by the $MnSO_4$ concentration; smaller particle and pore sizes are observed with a more diluted solution.

SEM images of the hollow nanospheres reveal that the nanospheres are composed of γ-MnO_2 hexagonal flakes arranged to form the surface of the nanospheres (Figure 3a−c). The available cations to balance the negative charge of the MnO_6 octahedra are protons because no other cations were used in the synthesis procedure. These acid sites in manganese oxide OMS materials are effective in catalyzing different reactions. An example is the selective oxidation of alcohols achieving both a high selectivity and a high conversion.[5,12]

TEM experiments confirmed that the structures were hollow and spherical as determined from microtomy and tilting experiments (Figure 4). High-resolution images were obtained in the direction perpendicular to the γ-MnO_2 flake (Figure 4c). A particle size distribution and selected area electron diffraction were performed and are shown in Figure 5; the average particle size was calculated to be 432 nm. In addition to the samples prepared by traditional powder techniques for the TEM studies, ultramicrotomy was also performed to determine shell thickness and to confirm that the nanospheres were hollow. However, compression of the hollow spheres occurs from the pressure of the glass knife in the direction of the cut.

The mechanism involved for the formation of the hollow structures is still unknown. One theory suggests that when the particles are formed, the interfacial tension and the hydrophilic surfaces of γ-MnO_2 play an important role in driving the nanoscale hexagonal flakes of γ-MnO_2 to form hollow structures. The nanospheres are stable up to 400 °C as confirmed by TGA, XRD, SEM, and BET. Greater than 400 °C, a mixed phase is observed (γ-MnO_2 and Mn_2O_3), and once the temperature reached 550 °C, only Mn_2O_3 exists. Additional changes at 400 °C include a 10% decrease in surface area and the observance of an additional pore size centered at 4 nm due to the removal of H_2O.

Initial catalytic studies have shown that the self-assembled structure of γ-MnO_2 is more catalytically active than the standard γ-MnO_2. The selective oxidation of cinnamyl alcohol to cinnamyl aldehyde was compared for standard γ-MnO_2 and the nanosphere γ-MnO_2. The typical γ-MnO_2 showed less than 10% conversion, whereas the nanosphere structure had a conversion of 42% with 95% selectivity under the same conditions.[5,12] In summary, mesoporous manganese oxide OMS materials with novel hollow nanosphere structures and uniform particle size were synthesized by a facile, template-free self-assembly process at room temperature in a short period of time. Using the hollow nanospheres as precursors, we have successfully obtained other manganese oxides OMS materials with different tunnel structures and morphologies (nanorods and 1D nanofibers).

Acknowledgment. We thank the Geosciences and Biosciences Division of the Office of Basic Energy Sciences, Office of Science, U.S. Department of Energy, Office of Basic Energy Science for support of this research and Dr. Frank Galasso for helpful discussions. We would also like to acknowledge Mr. Jim Romano and Steve Daniels for providing access to their TEM and FESEM facilities in the Department of Physiology and the Neurobiology Department, UConn, Mark Aindow for use of the JEOL 2010 TEM in the Institute of Materials Science, UConn, as well as Young-Chan Son for his help with the catalysis.

References

(1) (a) *Hollow and Solid Spheres and Microspheres: Science and Technology Associated with Their Fabrication and Application*; Wilcox, D. L., Berg, M., Bernat, T., Kellerman, D., Cochran, J. K., Eds.; MRS Symposium Proceedings, Vol. 372; Materials Research Society: Pittsburgh, PA, 1995. (b) Caruso, F. *Adv. Mater.* **2001**, *13*, 11.

(2) (a) Wang, D.; Caruso, R. A.; Caruso, F. *Chem. Mater.* **2001**, *13*, 364. (b) Kulinowski, K. M.; Harsha, V.; Colvin, V. L *Adv. Mater.* **2000**, *12*, 833. (c) Han, S.; Sohn, K.; Hyeon, Y. *Chem. Mater.* **2001**, *13*, 2337.

(3) (a) Lee, J.; Sohn, K.; Hyeon, T. *J. Am Chem. Soc.* **2001**, *123*, 5146. (b) Liu, T.; Wan, Q.; Xie, Y.; Burger, C.; Liu, L.; Chu, B. *J. Am. Chem. Soc.* **2001**, *123*, 10966.

(4) (a) Chabre, Y.; Pannetie, J. *Prog. Solid State Chem.* **1995**, *23*, 1. (b) Giraldo, O.; Brock, S.; Marquez, M.; Suib, L. S. *J. Am. Chem. Soc.* **2000**, *122*, 9330.

(5) Son, Y.; Makwana, V.; Howell, A. R.; Suib, L. S. *Angew. Chem., Int. Ed.* **2001**, *40*, 4280.

(6) (a) Shen, Y. F.; Zerger, R. P.; DeGuzman, R. N.; Suib, S. L.; McCurdy, C. L.; Porter, D. I.; O'Young, C. L. *Science* **1993**, *260*, 511. (b) Luo, J.; Suib, S. L. *J. Phys. Chem. B* **1997**, *101*, 10403.

(7) (a) De Wolff, P. M. *Acta Crystallogr.* **1959**, *12*, 341. (b) Giovanoli, R. 2nd International Symposium on Manganese Dioxide; Tokyo, Japan, Oct. 27−29, 1980; p 177.

(8) Zhang, Q. Doctoral Dissertation, University of Connecticut, Storrs, CT, 2001.

(9) (a) Preisler, E. *J. Appl. Electrochem.* **1989**, *19*, 540. (b) Ruetschi, P.; Giovanoli, R. *J. Electrochem. Soc.* **1988**, *135*, 2663. (c) Andersen, T. N. *Prog. Batteries & Battery Mater.* **1992**, *11*, 105.

(10) Kotai, L.; Keszler, A.; Pato, J.; Holly, S.; Banerji, K. K. *Indian J. Chem., Sect. A* **1999**, *38A*, 966.

(11) Ertl, G. In *Handbook of Heterogeneous Catalysis*; Ertl, G., Knèozinger, H., Weitkamp, J., Eds.; Wiley-VCH: Weinheim, 1997; p 432.

(12) Son, Y. C.; Makwana, V. D.; Howell, A. R.; Suib, S. L. *Angew. Chem.* **2001**, *113*, 4410.

JA0294459